Deep Neural Networks Methods For Estimating Market Microstructure and Speculative Attacks Models : The Case of Government Bond Market

DAVID ALAMINOS

MARÍA BELÉN SALAS

MANUEL A. FERNÁNDEZ-GÁMEZ

A sovereign bond market offers a wide range of opportunities for public and private sector financing and has drawn the interest of both scholars and professionals as they are the main instrument of most fixed-income asset markets. Numerous works have studied the behavior of sovereign bonds at the microeconomic level, given that a domestic securities market can enhance overall financial stability and improve financial market intermediation. Nevertheless, they do not deepen methods that identify liquidity risks in bond markets. This study introduces a new model for predicting unexpected situations of speculative attacks in the government bond market, applying methods of deep learning neural networks, which proactively identify and quantify financial market risks. Our approach has a strong impact in anticipating possible speculative actions against the sovereign bond market and liquidity risks, so the aspect of the potential effect on the systemic risk is of high importance.

Keywords:

Government bond; public debt; speculative attacks; deep neural networks; market micro-structure; systemic risk.

1. Introduction

Government bonds are the main instrument of most fixed income asset markets, for developed and developing economies alike. They supply a yield curve benchmark and help set the global credit curve across countries. In the United States, the main data source for public securities trading activity is GovPX and MTS for Europe. The MTS is a fully electronic, quote-driven interbank market comprising multiple trading platforms. All MTS platforms use identical technology for trading; however, every platform maintains its rules set, market participants (Biais and Green, 2019; Friewald and Nagler, 2019). Fixed income securities are commonly traded over-the-counter (OTC), on inter-dealer wholesale platforms, and, less frequently, on retail platforms where liquidity is provided by pre-purchased dealers. Transactions are not anonymous and are bilateral; therefore, the conditions of negotiation are determined by search and trading frictions, in the absence of a focal point, dealers have to proactively seek out and negotiate with possible counterparties to get the "best" offer (Darbha and Dufour, 2013; Neklyudov, 2019; Glode and Opp, 2020). OTC markets draw significant volumes of trading despite the fragmentation that does not exist in the centralized limit order markets. However, given the significance of OTC in world financial marketplaces, the OTC market microstructure remains poorly known, due to both the scarcity of empirical data and the complexity of this diffuse and nontransparent dealing system (Back *et al.*, 2019; Issa and Jarnecic, 2019).

The numerous serious incidents of financial turbulence that have affected the world economy over the last 10 years have given rise to growing demands for stronger and closer involvement of governments in the financial market pricing procedure (Pasquariello *et al.*, 2020). A well-functioning and effective public debt market is, therefore, generally perceived to be relevant for the proper working of financial systems in general (Pholphirul, 2009; Bai *et al.*, 2013; International Monetary Fund, 2021). On the microeconomic policy level, the expansion of a national capital market can enhance financial stability overall and contribute to better financial intermediation by increasing competition and developing related financial infrastructure, services and products (Bessembinder *et al.*, 2020; Yurastika and Wibowo, 2021). According to Darbha and Dufour (2013), the main research areas of microstructure are liquidity, the formation of prices, trading costs and the impact of regulatory changes on the behavior of operators. They conclude that the costs of requiring prompt execution of transactions in fixed income markets, and the impact of trades on prices, can provide information to decision-makers on the effect of policy actions on the weakness of credit systems. These costs are a function of the volatility of yields, the arrival rates of customers and the likelihood of information distortions against intermediaries that provide liquidity (Piesse *et al.*, 2007; Ehrmann and Fratzscher, 2017).

Although government bonds are often viewed by market participants as safe and liquid assets, Pelizzon *et al.* (2013) showed that the state debt securities proved not to be insensitive to the cash crunch. When market participants required liquidity, they started to sell off any of their most highly liquid assets, spreading the liquidity crisis even to government bonds. Therefore, governments should develop tools for liquidity risk management and apply them to fixed income markets (Fleming *et al.*, 2018; Benos *et al.*, 2019; Schlepper *et al.*, 2020; Pasquariello *et al.*, 2020). They investigate the impact of non-informative operations by central bankers on the government bond markets' liquidity in a context of both informed and policy speculation. They conclude that higher levels of uncertainty aggravate equilibrium market liquidity because they make private information of speculators more high-value and the attendant more stringent negative screening risk for

market-makers. They, therefore, proposed as future research a government bond model that considers the incidence of market manipulation by speculators.

On the other hand, speculative attacks cause major disruptions in the government bond market, playing a major factor in sparking shifts in the market's microstructure (Biais and Green, 2019). Speculative attack models were successfully implemented in a diverse variety of crises. Fujimoto (2014) concluded that although his research has focused on the currency crisis scenario, its wider implications span a broader framework and that future research requires a different approach to other markets. Some authors have investigated price speculation in the government bond market (Carfì and Lanzafame, 2013; Della Posta, 2016, 2021). According to Della Posta (2016), speculators assess the condition of the debt to determine if a selling attack on it is beneficial or not, while borrowers evaluate the benefits and costs of abandoning the initial commitment to repay their debt. Della Posta (2021) showed that the primary surplus that must be achieved to ensure government debt is stable and can be constrained by a higher limit of viability, thus establishing a higher limit on the rate of interest that ensures the stability of government debt as well. It is the absence of a credible upper limit that is behind the speculative assault on sovereign debt. Hence, financial organizations and policy makers need to understand how the bond market works to formulate the regulation in this system and estimate potential systemic risks. If speculative financial market conduct is concentrated on sovereign government debt, it is up to the government to make the best decision, i.e., whether to default on government debt, considering the benefits and expenses of default and what kind of economic policy to adopt to reduce the probability of a speculative attack (Della Posta, 2016). The increasing difficulty of economic decisions, particularly in financial markets, means that new methodologies are needed to estimate speculative attack models with greater precision and to prevent liquidity risks, as these models have almost always been estimated using statistical techniques (Benchimol and Fourçans, 2017).

To fill this gap and given the importance of the incidence of market manipulation by speculators, this research builds different machine learning techniques for predicting speculative attacks in the fixed income asset markets, specifically with government bonds. For this purpose, we have analyzed data for the two countries, Greece and Thailand, both of which have struggled in recent decades with the problems of the Greek sovereign debt crisis and the yield volatility in the Thai bond market, having an impact on liquidity, and being subject both countries to attacks by numerous players in the state securities market. The method used is that of Deep Neural Networks, specifically Convolutional Neural Network (CNN), Recurrent Convolutional Neural Network (RCNN) and Long Short-Term Memory (LSTM) verifying that it may be the best methodology to detect and predict this type of unexpected situations, offering greater robustness in their results. The models that have been built using this methodology are as follows: liquidity measure coupon, liquidity measure CDS, time-weighted bid-ask spread (TWBAS), volatility, large versus small players and arbitrage no feasibility equation. Deep Neural Networks methods have been extensively employed in a variety of computational problems (predicting energy prices, processing of data and macro/micro tendency analysis, forecasting of demand, administration of risks, negotiation skills) that generally face the difficulty known as the curse of

dimensionality. Therefore, the remarkably superior results obtained using the reported methods suggest that they can be effectively implemented in such difficult computational problems (Inglada-Pérez, 2010). As market turmoil and uncertainty in financial markets have increased considerably, machine learning algorithms are quite applicable for the analysis of financial markets and, in particular, the sovereign bond market. Financial disorder emerges if financial circuits are susceptible to early state conditions and produce unpredictable long-term effective behavior, driven by natural events and spillover factors, such as speculative attacks (Horváth *et al.*, 2006; Klioutchnikov *et al.*, 2017). The marketplace is very complicated, and the only forecast that can be made is its unpredictability. The financial market's unforeseeability is caused by the uncertainty of many episodes that occur in it. Deep Neural Networks draw knowledge from the data, which can then be utilized to forecast and produce further data. This feedback decreases unreliability by indicating specific problem-solving. Machine learning is especially useful for handling problems where an analytical solution is not explicitly instructed to do so, such as complete categorization techniques or recognition of trends (Ghoddusi *et al.*, 2019). Therefore, our new model, developed using machine learning techniques, will be useful in detecting and forecasting the speculative reaction of financial markets on public debt.

The contribution of our study is that we have obtained high levels of accuracy in our models, thanks to new estimation techniques we have considered, achieving high performance and precision. The benefit of Deep Neural Network methods over those offered by classical statisticians and econometricians is that machine learning algorithms can handle a huge quantity of organized and nonstructured information and provide quick predictions or conclusions (Ghoddusi *et al.*, 2019), improving the real market detention of scenarios of speculative attacks. Therefore, our method is a powerful way to explain and predict the behavior of financial markets, being able to detect trends that are at the root of the uncertainty, solidity or disorderly chaos of a financial system (Klioutchnikov *et al.*, 2017). Therefore, our model provides a complex quantum study, being a reliable solution to contemplate the uncertainty and complexity of the financial system, the aim being to simulate speculative attack models to provide more information about the possible events that may occur in the state securities market.

This paper is arranged as follows. In Section 2, the methodology is described. Section 3 details the estimation methods. Section 4 shows all data used for the study. Section 5 points out the results and findings obtained. Section 6 concludes.

2. Methodology

2.1. *Speculative attacks' model*

Since the success of the attack is decided in period 2, we first consider the small players' actions from period 1 and then consider the big player's decision whether or not to start an early attack. A possible delayed strike by the big investor would be the rest of his L-credit following any speculation advanced on.

According to Corsetti *et al.* (2004), we will suppose that the small players play an activation strategy where agents assail the coin if the symbol drops under a certain value x^*.

Like in this approach the equilibrium unique to the model is defined by two crucial variables: x^* and a fundamental minus crucial parameter for early speculation by the big investor, $(\theta-\lambda)$. If $\theta-\lambda \leq (\theta-\lambda)^*$, the coin would collapse.

We first discuss the equilibrium of the given activation strategies; we, therefore, examine the optimal strategies for activation. Certainly, if the approach is activated, a minor agent i would attempt to raid the coin if his signal $x_i \leq x^*$. The likelihood of occurrence depends on the true economic situation, $\theta-\lambda$, described as follows:

$$\begin{aligned}\text{prob}[x_i \leq x^* | \theta-\lambda] &= \text{prob}[\theta-\lambda+\sigma\varepsilon_i \leq x^*] = \text{prob}\left[\varepsilon_i \leq \frac{x^*-(\theta-\lambda)}{\sigma}\right] \\ &= F\left(\frac{x^*-(\theta-\lambda)}{\sigma}\right). \end{aligned} \tag{1}$$

Because there is a small-agent continuum, and their noise conditions are separate, a joint confusion about the conduct of little actors is absent. Therefore, the density of attacking minor agents, ξ, is the same as this probability. Since $F(.)$ is tightly rising, the impact of the conjectural attack is narrowly declining in $\theta-\lambda$; the weaker the big investor's early speculation, the further little agents will strike.

A successful speculative attack would occur if the aggregate of minor speculative actors outweighs the power of the economic fundamentals, minus the speculation early on by the big actor, i.e., if

$$F\left(\frac{x^*-(\theta-\lambda)}{\sigma}\right) \geq \theta-\lambda. \tag{2}$$

Hence, the crucial variable $(\theta-\lambda)^*$, for the set of minor actors attacking is enough to provoke a devaluation, as follows:

$$F\left(\frac{x^*-(\theta-\lambda)^*}{\sigma}\right) = (\theta-\lambda)^*. \tag{3}$$

For smaller amounts, in which $\theta-\lambda \leq (\theta-\lambda)^*$, the impact of speculation is higher, and the force of the exchange rate fixed smaller, which implies that aggression has more success. Consequently, for greater parameters, where $\theta-\lambda > (\theta-\lambda)^*$, the occurrence of speculation is shorter and the fixed exchange rate force higher, meaning that an assault would not have success.

We obtain the activation-optimal approaches of the minor actors. An investor notices a signal x_i and, for this signal, the likelihood of a successful offense is denoted by

$$\begin{aligned}\text{prob}[\theta-\lambda \leq (\theta-\lambda)^* | x_i] &= \text{prob}[x_i-\sigma\varepsilon_i \leq (\theta-\lambda)^*] = \text{prob}\left[\varepsilon_i \geq \frac{x_i-(\theta-\lambda)^*}{\sigma}\right] \\ &= 1-F\left(\frac{x_i-(\theta-\lambda)^*}{\sigma}\right) = F\left(\frac{(\theta-\lambda)^*-x_i}{\sigma}\right), \end{aligned} \tag{4}$$

where the last equation is derived from $f(.)$, $F(\nu) = 1 - F(-\nu)$. The reward requested from hitting the coin for agent i, by speculation value, is therefore

$$(1-t)F\left(\frac{(\theta-\lambda)^* - x_i}{\sigma}\right) - t\left(1 - F\left(\frac{(\theta-\lambda)^* - x_i}{\sigma}\right)\right) = F\left(\frac{(\theta-\lambda)^* - x_i}{\sigma}\right) - t. \quad (5)$$

In an activation optimal strategy, the reward anticipated of the coin attack for the marginal player has to be equal to 0, the best cut x^* in the activation, the approach is provided by

$$F\left(\frac{(\theta-\lambda)^* - x^*}{\sigma}\right) = t. \quad (6)$$

To resolve the balance, we redesign (6) to get $(\theta-\lambda)^* = x^* + \sigma F^{-1}(t)$. Replacing into (3), we obtain

$$\begin{aligned} (\theta-\lambda)^* &= F\left(\frac{x^* - (x^* + \sigma F^{-1}(t))}{\sigma}\right), \quad \text{or} \\ (\theta-\lambda)^* &= F(-F^{-1}(t)) = 1 - F(-F^{-1}(t)) = 1 - t. \end{aligned} \quad (7)$$

So, these parameters are

$$(\theta-\lambda)^* = 1 - t \quad \text{and} \quad (8a)$$

$$x^* = 1 - t - \sigma F^{-1}(t). \quad (8b)$$

These parameters match with the only novelty being the early speculation of the major agent λ.

Next, we take into account the big player's decision whether or not to speculate in period 1, and, if so, to what extent. There is no incertitude in the small players' combined behavior, hence the large player can perfectly predict its speculation, save for the noise of its sign. From (8), there will be a devaluation if the essential $\theta \le \theta^* \equiv 1 - t + \lambda$.

The likelihood of aggression being successful can be expressed as

$$\begin{aligned} \text{prob}[\theta \le 1 - t + \lambda | y] &= \text{prob}[y - \tau\eta \le 1 - t + \lambda | y] = \text{prob}\left[\frac{y - \lambda - (1-t)}{\tau} \le \eta | y\right] \\ &= G\left(\frac{1 - t + \lambda - y}{\tau}\right), \end{aligned} \quad (9)$$

where we once again employ the distribution symmetry. If the attack is successful, the major investor also wishes to build up speculation in the next period, so that the total amount of speculation is L. But we have the risk, which occurs with quantity q, that speculation in the next period is much excessively delayed, hence the big investor benefits only from his speculating early λ. The payoff desired to attack in quantity $\lambda \ge 0$ in an early phase is, therefore,

$$E\pi = G\left(\frac{1 - t + \lambda - y}{\tau}\right)(L(1-q) + \lambda q) - t\lambda. \quad (10)$$

The first requirement for an indoor explanation λ^* is

$$\frac{\partial E\pi}{\partial \lambda} = g\left(\frac{1-t+\lambda^*-y}{\tau}\right)\frac{1}{\tau}(L(1-q)+\lambda^* q) + G\left(\frac{1-t+\lambda^*-y}{\tau}\right)q - t = 0. \quad (11)$$

Since $E\pi$ is a function uninterrupted of λ, which is fixed on the closed interval $[0, L]$, we assume the existence of an early optimum quantity of speculation λ, which maximizes the profit expectation. Yet, the optimum λ is neither single nor internal. Indeed, if speculation charges, t, are low, the efficient speculation soon is the same as the L credit constraint.
Rule 1. Requirements for speculation at an early stage by major investors:

There is a value critical to the charges of early speculation $\underline{t} > 0$ as if $0 < t < \underline{t}$, for certain values of the other parameters, indicating that the efficient early speculation is the higher restriction, $\lambda = L$. For some variables of other indicators, there is a score to the charges of speculation $\bar{t} > 0$ as if $t > \bar{t}$, this means that the efficient early speculation becomes 0, $\lambda = 0$.

So, if speculation is very low, as speculation encourages minor agents to assault, it is the more lucrative option. Since the major actor is a neutral risk, then he will hypothesize up to his boundary L. But, if speculation is costly enough, it would at no time be worth speculating at an early stage.

The second condition if the solution is internal is

$$\frac{\partial^2 E\pi}{\partial^2 \lambda} = g'\left(\frac{1-t+\lambda^*-y}{\tau}\right)\frac{1}{\tau^2}(L(1-q)+\lambda^* q) + 2g\left(\frac{1-t+\lambda^*-y}{\tau}\right)\frac{q}{\tau} < 0. \quad (12)$$

The second term of (12) is a positive term, which implies that the first terminus should be contradictory, for example, that $g'(.) < 0$ in an internal solution. To investigate the impact of rising costs of speculation t on the efficient speculation, note that (11) could be denoted by $H(\lambda, t) = 0$, which implies the definition of the efficient speculation λ^* to be a function of costs of speculation. Deferring about t, we get $H_1 \frac{d\lambda^*}{dt} + H_2 = 0$, or $d\lambda^*/dt = -H_2/H_1$, where $H_2 \equiv \frac{\partial^2 E\pi}{\partial \lambda \partial t}$ and $H_1 \equiv \frac{\partial^2 E\pi}{\partial^2 \lambda} < 0$ from the second requirement. It deduces, thus, that the sign of $\frac{d\lambda^*}{dt}$ is the same as the sign of $H_2 \equiv \frac{\partial^2 E\pi}{\partial \lambda \partial t}$. We distinguish the first-order condition (11) about t, leading to

$$\frac{\partial^2 E\pi}{\partial \lambda \partial t} = -g'\left(\frac{1-t+\lambda^*-y}{\tau}\right)\frac{1}{\tau^2}(L(1-q)+\lambda^* q) - g\left(\frac{1-t+\lambda^*-y}{\tau}\right)\frac{q}{\tau} - 1. \quad (13)$$

A rise in speculation charges t concerns efficient early speculation through the three terms in (13), with the second and third terms being refusal. The reduction in speculation by minor investors due to upper charges of speculation is reflected in the second term. This decreases the success likelihood of the assault, and thus decreases the estimated return on the early speculation. The third variable incorporates the impact of greater speculation rates, making speculation more costly, and driving less speculation early on.

For the very first term, though, it assumes that it is affirmative, since $g'(.) < 0$. As greater speculation costs decrease speculation by minor agents, the projected impact of greater early speculation by the major player on the probability of success rises.

The phenomenon encourages the big trader to expand early speculation. Indeed, it is not excluded that this mechanism may dominate for some range of t, which implies that an increment in speculation charges can induce an increase in speculation by the large trader.

The model might be changed to accept $N > 1$ major traders as described below. First, for tractability reasons, it will disregard information imbalances between the large investors, under the assumption that all of them are observing the identical signal y. These are companies that devote a significant number of funds to the market and have available similar information feeds, so can be a reasonable approximation neglecting information asymmetries. Next, it presumes that the prices of speculation fundings are convex, implying that the charges of speculation λ_j for agent j is $tc(\lambda_j)$, for which $c(.)$ is convex and strongly positive. The estimated profit from the speculation of player j will be $E\pi_j = G(\frac{1-t+\lambda-y}{\tau})(L_j(1-q)+\lambda_j q) - tc(\lambda_j)$ where $\lambda = \sum_j \lambda_j$, and L_j is player j's credit limit. It follows from the above pattern arguments that a Nash equilibrium exists in combined approaches to the speculation by major agents, but unanimity is not assured. However, similar results to Rule 1 can be deduced, which implies that if costs are not above a critical value, there will be no speculation. The first requirement for efficient indoor speculation λ_j^* of agent j is

$$\frac{\partial E\pi}{\partial \lambda_j} = g\left(\frac{1-t+\lambda^*-y}{\tau}\right)\frac{1}{\tau}(L_j(1-q)+\lambda_j^* q) + G\left(\frac{1-t+\lambda^*-y}{\tau}\right)q - tc'(\lambda_j^*) = 0. \tag{14}$$

In an equilibrium interior in pure strategies, all major traders would soon speculate in the quantity shown by (14).

2.2. *The state bond interest rate and its higher ceiling*

2.2.1. *The interest rate on state bonds*

A variant of the interest rate differential to government bonds in a linearized form is given in the following equation:

$$i_t = \bar{r} + RP_t, \tag{15}$$

where

$$RP_t = \alpha b_t + \beta \frac{E(di_t)}{d_t}, \tag{16}$$

so that

$$i_t = \bar{r} + \alpha b_t + \beta \frac{E(di_t)}{d_t}. \tag{17}$$

Equation (15) states that the interest rate, i_t, could be considered to be given by a risk-free benchmark interest rate, $\bar{r}$ and by a risk prime, RP_t. The latter relies on two factors recognized in the relevant studies, as shown in (16). The first is the ratio of government debt to GDP, because the larger b_t is, the lower the estimated negative shocks to the

economy are likely to be (Corsetti *et al.*, 2014). The parameter α measures the interest rate sensitivity concerning b_t. On the other hand, the second part has characteristics of self-fulfillment. The smaller the projected acceptability of government debt, the larger the anticipated interest rate change in the future, which one after another impacts the present interest rate' domain with a value assigned by the value of the setting β.

2.2.2. *The higher interest rate ceiling of the government bond yields*

Government and central bank, which are both operating via the instrument under their control, $\bar{r}$, and using the possible monetization of public debt must comply with a higher level of nominal yields on government debt to ensure the sustainability of public bonds.

The interest rate also has a minimum value, which can be regarded as the zero lower bound (though central banks have proven that it is possible to go even below it). The value assumed by i_t, may then be labeled, as shown in the following way:

$$\begin{aligned} i_t &= \bar{i}^* \quad \text{if } i_t \geq \bar{i}^*, \\ i_t &= \tilde{i}_t \quad \text{if } \underline{i}^* < i_t < \bar{i}^*, \\ i_t &= \underline{i}^* \quad \text{if } i_t < \underline{i}^*, \end{aligned} \tag{18}$$

where $\bar{i}^*$, $\underline{i}^*$, $\tilde{i}_t$ and i_t denote, simultaneously, the higher and lower limits for the interest rate, the rate of interest that could be achieved if it moves inside the announced ranges and the interest rate that remains in the event of noncommitment, where $\bar{i}^*$ is a simplicity value fixed by the public debt adequacy equation, as explained next.

The typical government debt developments, i.e., the changes in government debt over time about GDP, db_t, when central government unanimity is not allowed — as is the euro zone — is given as follows:

$$db_t = f_t dt - m_t dt + (i_t - g_t) b_t dt + \sigma dz. \tag{19}$$

The factor f_t is the ratio of the primary government deficit to GDP (i.e., $e_t - t_t$, where e_t is government fiscal spending relative to GDP and t_t are public revenues about GDP) and m_t is the rate of monetization of government debt (Tamborini, 2015). The expression $(i_t - g_t)b_t$ is the debt service as a share of GDP. The component stochastic of the growth of state debt relative to GDP is assumed to pursue a Brownian cycle σdz. The character σ stands for the standard deviation of the Brownian cycle and dz is the variation of the Brownian movement, defined as follows:

$$dz = \chi \sqrt{dt}, \tag{20}$$

where χ is a probability variable that is normally, separately and equally dispersed, with average 0 and variance is 1, and dt is infinity time-varying variation.

Setting $db_t = 0$ in (19), and supposing that $m_t = 0$, it results that the long-term primary surplus/deficit must provide for the long-run service on the debt:

$$f^* = (g^* - i^*)\bar{b}, \tag{21}$$

referring the symbol * to long-term securities.

If $i^* > g^*$, for $(g^* - i^*) < 0$, it implies that $f^* < 0$, the state requires a surplus on the budgetary position $s^* = -f^*$ to balance public debt.

Therefore, reordering (21), gets the following:

$$i^* = g^* + \frac{s^*}{\bar{b}}, \tag{22}$$

where i^* denotes the long-term interest rate which ensures a ratio of government debt to GDP, $\bar{b}$, for a specified long-term main excess, s^* and a long-term rate of GDP increase, g^*.

The primary surplus a government could implement is not limitless (Tamborini, 2015). It is measured by applying a comparison of the solvency cost (related positively to s^*) and the cost of nonpayment (linked negatively to s^*), in such a way that it is defined at the moment when the two are equal. The maximum achievable long-run primary surplus of the government is denoted by s^*. This highest possible feasible $\bar{s}^*$, in fact, sets $\bar{i}^*$, that is the highest long-term interest rate that a government can allow to spend on its sovereign debt to guarantee its viability. For the sustainability of government debt to be viable, it implies that $s^* \leq \bar{s}^*$, which means that $i^* \leq \bar{i}^*$.

Thus, the i^* that the government (which has to cope with $\bar{s}^*$) may plausibly argue for is given by

$$\bar{i}^* = g^* + \frac{\bar{s}^*}{\bar{b}}. \tag{22'}$$

Whereas (15) and (22′) mean

$$\overline{RP}^* = g^* + \frac{\bar{s}^*}{\bar{b}} - \bar{r}^*, \tag{22''}$$

where $\overline{RP}^*$ captures the largest risk premium that a government can bear for a certain $\bar{s}^*$, $\bar{r}^*$, $g^*$to maintain $\bar{b}$ at its constant value of the country. The variable $\bar{r}^*$ is the smallest level of the central bank's choice of long-term interest rate and still guarantees the solidity of government debt.

Remember, though, that so far we have supposed that $m_t = 0$, an assumption that means that there is no creditor of the final instance. If the central bank is in a position to pay off government debt, in the context of stochastic crises, a monetary debt smoothing mechanism would open up, combined with that generated by the fiscal authority's primary surplus, as we will examine in the following discussions.

2.3. *The interest rate objective framework*

Government settles sovereign debt in the stationary condition for a certain maximal achievable value of $\bar{s}^*$, g^* and $\bar{i}^*$, as discussed above. However, this levelling off does not exclude other changes in sovereign debt. This implies that sovereign debt as a percentage of GDP could continue to get up, given the stochastic shock process to which it may be exposed:

$$db_t = \sigma dz. \tag{23}$$

The implication of this is that public debt may continue to rise beyond its stationary status value and this could raise the risk prime over the amount that the public government could bear to ensure the creditworthiness of the public debt.

This is because there is no more scope for defending the government's debt stability, i.e., neither additional government primary surpluses are achievable, nor is the central bank able or prepared to ensure the rise in the interest rate than $\bar{i}^*$: such is the scenario if $s^* > \bar{s}^*$

If on the other hand the government is required to supply the primary surplus (achievable), needed to ensure the government's debt stability and/or if the central bank responds by purchasing government debt to sustain the price of bonds with its demand, such that $m_t > 0$, the interest rate may easily stay inside the belt $\tilde{i}_t < \bar{i}^*$. The interest rate could, therefore, settle, and this would lead to a "honeymoon" as described by Krugman (1991).

In summary, this public debt model is made up of the next two equations, mentioned before:

$$i_t = \bar{r} + \alpha b_t + \beta \frac{E(di_t)}{d_t}. \tag{23'}$$

$$db_t = \sigma dz \tag{23''}$$

This system is quite reminiscent of Krugman's (1991) original target area model, further modified by Bertola and Caballero (1992).

To resolve (23″) and (23), we use the literature on target areas assembling a general form for $\tilde{i}_t$, with b_t as a function. Noting (23″), we may consider $\tilde{i}_t$ as a function of the debt/GDP ratio

$$\tilde{i}_t = q(b_t). \tag{24}$$

We may apply this equation to compute the assumed change in the interest rate. To do this, we extend this equation in a Taylor-type series, estimating Ito's spread:

$$d\tilde{i}_t = q'(b_t)E(db_t) + \frac{1}{2}q''(b_t)E(db_t)^2. \tag{25}$$

According to the definition of db_t in (23), it follows that $(db_t)^2 = \sigma^2\chi^2 dt$. Taking the predicted values and dividing by the time variation infinitesimal, we get Ito's lemma:

$$\frac{E(d\tilde{i}_t)}{d_t} = \frac{1}{2}q''(b_t)\sigma^2, \tag{26}$$

since $\frac{E(db_t)}{dt} = 0$ and $\frac{E(db_t)^2}{dt} = \sigma^2$. Substituting (26) into (19′), we get

$$\tilde{i}_t = q(b_t) = \bar{r} + \alpha b_t + \beta\frac{1}{2}q''(b_t)\sigma^2. \tag{27}$$

This is a second-order differential equation, for which the generic form of the solution is as follows:

$$\tilde{i}_t = q(b_t) = \bar{r} + \alpha b_t + A_1 e^{\lambda_1 b_t} + A_2 e^{\lambda_2 b_t}. \tag{28}$$

Consider the second-order derivative of (28) to get a score corresponding to

$$q''(b_t) = \lambda_1^2 A_1 e^{\lambda_1 b_t} + \lambda_2^2 A_2 e^{\lambda_2 b_t}. \tag{29}$$

So, substituting it into (27), we get

$$\tilde{i}_t = q(b_t) = \bar{r} + \alpha b_t + \beta \frac{\sigma^2}{2} (\lambda_1^2 A_1 e^{\lambda_1 b_t} + \lambda_2^2 A_2 e^{\lambda_2 b_t}). \tag{30}$$

Matching (30) with (28), we get

$$\begin{aligned} &A_1 e^{\lambda_1 b_t} + A_2 e^{\lambda_2 b_t} = \beta \frac{\sigma^2}{2} (\lambda_1^2 A_1 e^{\lambda_1 b_t} + \lambda_2^2 A_2 e^{\lambda_2 b_t}), \\ &A_1 e^{\lambda_1 b_t} \left(\lambda_1^2 \beta \frac{\sigma^2}{2} - 1 \right) + A_2 e^{\lambda_2 b_t} \left(\lambda_2^2 \beta \frac{\sigma^2}{2} - 1 \right) = 0, \\ &A_1 e^{\lambda_1 b_t} \left(\lambda_1^2 \beta \frac{\sigma^2}{2} - 1 \right) = 0, \quad \text{and} \quad A_2 e^{\lambda_2 b_t} \left(\lambda_2^2 \beta \frac{\sigma^2}{2} - 1 \right) = 0. \end{aligned} \tag{31}$$

We can now obtain λ_1 and λ_2 by resolving the next two equations:

$$\left(\lambda_1^2 \beta \frac{\sigma^2}{2} - 1 \right) = 0 \quad \text{and} \quad \left(\lambda_2^2 \beta \frac{\sigma^2}{2} - 1 \right) = 0.$$

As a solution, we get

$$\lambda_{1,2} = \pm \sqrt{\frac{2}{\beta \sigma^2}}. \tag{32}$$

This implies that we obtain two complimentary solutions that fulfil the second-order differential equation: $\tilde{i}_t^{c1} = A_1 e^{\lambda_1 b_t}$ and $\tilde{i}_t^{c2} = A_2 e^{\lambda_2 b_t}$.

We sum them to derive the general solution, with λ_1 and λ_2 described as high-up:

$$\tilde{i}_t = q(b_t) = \bar{r} + \alpha b_t + A_1 e^{\lambda_1 b_t} + A_2 e^{\lambda_2 b_t}.$$

Ignoring the bottom (implicit) band, thus excluding the A_2 coefficient (the convenience of this supposition, which is not required and is only used to concentrate on the upper boundary behavior, could be further corroborated because the zero lower limits no longer appears to be mandatory, as national central banks are now even targeting negative interest rates). Define, then, the fixed value A_1.

The expectation that the present rate of interest, $\tilde{i}_t$, will not be able to surpass the level $\bar{i}^*$, is driven by the anticipation that $\tilde{i}_t$ will be lowered by a decrease in b_t, which is made possible by a larger primary surplus and/or via a decrease in public debt held by the private sector due to stronger demand from the central bank. Thus, when $\tilde{i}_t$ catches up to $\bar{i}^*$, the first is unlikely to be exceeded by it, so it will stay within the band, regardless of if b_t is rising or falling: this is only possible if there is a tangency order.

Thus, we apply the condition of "soft sticking" to the above equation:

$$\frac{d\tilde{i}_t}{db_t} = \alpha + \lambda_1 A_1 e^{\lambda_1 b_t} = 0. \tag{33}$$

It can be seen from this that

$$A_1 = \frac{-\alpha e^{-\lambda_1 b_t}}{\lambda_1} < 0. \tag{34}$$

Then, we get

$$\tilde{i}_T = \bar{r} + \alpha \bar{b} - \frac{\alpha}{\lambda_1}. \tag{35}$$

It also happens to

$$b_T = \bar{b} + \frac{1}{\lambda_1}, \tag{36}$$

where $\bar{b} = \frac{\bar{i}^* - \bar{r}^*}{\alpha}$ is the ratio of government debt to GDP resulting when the interest rate attains $\bar{i}^*$ in its straight course, not suffering from the enforcement of the top end of the range. Taking that at time T, $\tilde{i}_T \leq \bar{i}^*$, substituting (32) into (36) (always with $A_2 = 0$) we get

$$b_T = \bar{b} + \frac{1}{\lambda_1} = \bar{b} + \sqrt{\frac{\beta\sigma^2}{2}}. \tag{37}$$

The discrepancy between b_T and $\bar{b}$, denoted by $\frac{1}{\lambda_1} = \sqrt{\frac{\beta\sigma^2}{2}}$, stands for what Krugman called the "honeymoon effect" and indicates by exactly how much it is likely to raise the sovereign debt to GDP ratio by holding $\tilde{i}_T \leq \bar{i}^*$.

What is suggested by the "soft sticking" condition is that the closer $\tilde{i}_t$ to $\bar{i}^*$, the more the main excess is supposed to rise, to ensure the supportability of sovereign debt (until it attains its maximum practicability restriction), and/or the more the central bank is likely to intercede by issuing government bonds, thus raising their price and lowering the interest rate below or at the limit of $\bar{i}^*$ Any raise in government debt due to stochastic shocks is thus expected to be offset by a higher surplus of government debt or by intervention by the central bank.

Nevertheless, the reverse result would be the case if there is an expected insufficient fiscal consolidation, as proposed by Tamborini (2015). In the euro zone crisis, Tamborini (2015) observed that in certain economies with increasing government debt, the primary surplus needed for a stable economy was nearing its upper limit of viability, at which no further stabilization was expected. The closer it approached $\bar{s}^*$, the less confidence there was in stabilization of sovereign debt and the more probable was the speculative attack, without a central bank to assume the lender of final instance role.

When $\tilde{i}_t$ reaches the interest rate level, $\bar{i}^*$ the first is permitted to rise over the second. As a reminder, this interest rate level is fixed to the upper limit of the main excess that the government can hold, fulfilling the stability of government debt. So, the upper the interest rate rises toward the end of the band, the greater the probability of reaching it.

It can be presumed that the ratio of government debt to GDP ranges between 0 and the maximum level of government debt ($\bar{b}$), resulting by the most practicable interest rate that ensures the solidity of the government debt ($\bar{i}^*$).

When the interest rate achieves its higher limit, $\bar{i}^*$, given the corresponding maximum level that government debt can achieve to be stable, $\bar{b}$, its value has to be the same as the expected value that results from the probability weights expected from the two different scenarios that can be expected to happen. A probability p exists that both governments do not have sufficient resources to prevent b_t from rising beyond $\bar{b}$, nor to prevent the interest rate from then exceeding its stable limit. This means that government debt can be permitted to overshoot its objective, and the interest rate will leap correspondingly.

The additional likelihood $(1-p)$ also exists, and that government debt does not rise, holding it at or below $\bar{b}$. The setting of the main excess at the margin could be such that its buoyancy band down by ϵ. Then, in this scenario, the government debt-to-GDP ratio will return to the center of a new way, $\bar{b}-\epsilon/2$, which lies intermediate from $\bar{b}-\epsilon$ and $\bar{b}$.

It follows that the arbitrage equation is shown:

$$p\tilde{i}_t\left(\bar{b}+\frac{\delta}{2},\bar{b}+\frac{\delta}{2}\right)+(1-p)\tilde{i}_t\left(\bar{b}-\frac{\epsilon}{2},\bar{b}-\frac{\epsilon}{2}\right)=\tilde{i}_t\left(\bar{b},\frac{\bar{b}}{2}\right), \tag{38}$$

where in the formula $\tilde{i}_t(xy)$, x denotes the actual value assumed by the fundamental, and y relates to the value given by the fundamental at the center of the band (Bertola and Caballero, 1992). Continuing with this by looking at a symmetric oscillation-band which is centered at point c and which implies that $A_1=-A_2$ and $\lambda_1=-\lambda_2$, the optimal control variable solution is

$$\tilde{i}_t=q(b_t,c)=\bar{r}+\alpha b_t+Ae^{-\lambda(b_t-c)}-Ae^{\lambda(b_t-c)}. \tag{39}$$

Consider, therefore, only one band, as in the example of "soft sticking":

$$\tilde{i}_t(b_t,c)=\bar{r}+\alpha b_t+Ae^{\lambda(b_t-c)}. \tag{40}$$

We get

$$p\left[\bar{r}+\alpha\left(\bar{b}+\frac{\delta}{2}\right)+A\right]+(1-p)\left[\bar{r}+\alpha\left(\bar{b}-\frac{\epsilon}{2}\right)+A\right]=\bar{r}+\alpha\bar{b}+Ae^{\frac{\bar{b}}{2}}, \tag{41}$$

it follows that

$$A=\frac{\left[p\alpha\left(\frac{\delta+\varepsilon}{2}\right)-\alpha\frac{\varepsilon}{2}\right]}{e^{\frac{\bar{b}}{2}}-1}. \tag{42}$$

This also signifies that $A\geq 0$ when $[p(\frac{\delta+\varepsilon}{2})-\frac{\varepsilon}{2}]\geq 0$, when

$$p\geq\frac{\varepsilon}{\delta+\varepsilon}, \tag{43}$$

corresponding to the Bertola and Caballero (1992) case for $\delta=\varepsilon=\bar{b}$. The insight behind this "divorce" outcome is fairly uncomplicated. The more government debt is assumed to raise as a result of stochastic shocks (the higher the δ), the smaller the p necessary for the interest rate to rise as a consequence of speculation. This, in time, relies on the missing expected resources to stabilize government debt, i.e., the absence of the ability to obtain the

main excess and/or the nonexistence of a central bank as a creditor of final instance. Certainly, the reverse is true for ε.

2.4. *Time-weighted bid-ask spread model*

The bid-ask spread, the liquidity measure most commonly used, is the distinction between the best bid and best offer published by liquidity providers. In applying the bid-ask spread, researchers compare spreads between securities using the proportional or relative differential, i.e., the bid-offer margin split by the middle point of the bid-offer quotations. Market makers mitigate transaction costs that emerge due to the risk of adverse selection, inventory handling, competition and order processing through quoting wide bid-ask spreads. Fleming (2003) examined various approaches to measure liquidity in the US Treasury market and determines that the bid-ask spread is the best indicator of liquidity. Beber *et al.* (2009) similarly employed the bid-ask spread as one of the cash measurements to investigate the effect of liquidity versus credit quality on sovereign yield differentials in the euro zone. Bid-ask spreads are generally good predictors of the execution cost of small trades, as large trades are often filled at lower prices or through negotiated settlements.

Market makers in MTS are instructed to deliver two-sided quotes for the majority of the trading day, but the quote updates are spaced irregularly over time, with periods of regular updates of contributions and then periods of delayed contribution updates. Hence, rather than simple averages of intraday spreads, time-weighted averages are employed. Intraday spreads are given weights based on the share of the day of trading on which they are open for trading before the next updating:

$$\mathrm{TWBAS}_d = \frac{1}{T}\sum_{t=1}^{Q}\frac{(\mathrm{Ask}_t - \mathrm{Bid}_t)}{(\mathrm{Ask}_t + \mathrm{Bid}_t)/2} * (T_{t+1} - T_t). \tag{44}$$

Time-weighted bid-ask spread TWBAS_d is a daily liquidity measurement estimated with all daily intraday revisions of the top bid and ask quotes; T_t is the time signature of the quote update expressed in seconds; Q is the total amount of quote reviews in a day, and T is the dealing day expressed in seconds.

Two alternative popular measures of the spread are the effective spread, described as the difference between the traded price and the midpoint of the spread, and the Roll spread, calculated from the covariance of consecutive price changes without the need for quote data. Bao *et al.* (2011) found that the Roll spread is better than the quoted bid-ask spread in explaining US corporate bond returns.

2.5. *Model for predicting volatility*

The volatility predicting is determined as in Qu *et al.* (2016), Haugom and Ullrich (2012) and Frömmel *et al.* (2014) as follows:

$$RV_t = \sum_{j=1}^{M} r_{t,j}^2, \tag{45}$$

being $j = 1, 2, \ldots, M$ in each day $t = 1.2$, and the jth intra-day return of day t is denoted as

$$r_{tj} = p_{tj} - p_{tj-1}, \tag{46}$$

where p_{tj} is the logarithmic price that is $p_{tj} = \log(P_t)$, being P_t the realized price.

To measure the return on our predictions, we use two commonly adopted metrics: mean absolute percentage error (MAPE) and root mean square error (RMSE). The formulas for these measures are as follows, with n being the data number to be predicted, y_t is the actual value of the data at time t and $\hat{y}_t$ is the actual value of y_t at time t. We employ the fitted form of the standard MAPE, suggested by Armstrong (1985) which is employed if the likelihood of the true values is equal to 0.

$$\text{MAPE} = \frac{1}{n} \sum_{t=1}^{n} \left| \frac{y_t - \hat{y}_t}{(y_t + \hat{y}_t)/2} \right|, \tag{47}$$

$$\text{RMSE} = \sqrt{\frac{\sum_{t=1}^{n} (y_t - \hat{y}_t)^2}{n}}. \tag{48}$$

2.6. *Liquidity measure model*

2.6.1. *Cross-sectional evidence*

We consider transversal regressions to investigate the determinants of liquidity in the market for government bonds. In particular, we examine whether each of our identified liquidity metrics could be estimated using the product features and dealing activity inputs. We estimate cross-sectional regressions in which we employ time-series means of all inputs. We test coupon bonds, according to the following regression:

$$\begin{aligned} \text{Coupon} : \text{LM}_i = {} & \beta_0 + \beta_1 \text{Age}_i + \beta_2 \text{AmountIssued}_i + \beta_3 \text{DailyTrades}_i \\ & + \beta_4 \text{CouponRate}_i + \beta_{5-8} \text{MaturityDummies}_i \\ & + \beta_9 \frac{\text{Time to Maturity}}{\text{Maturity}_i} + \beta_{10} \left(\frac{\text{Time to Maturity}}{\text{Maturity}_i} \right)^2 + \epsilon_i, \end{aligned} \tag{49}$$

where LM_i is the ith measurement of liquidity. Maturity is fixed as the time, in years, from the issue date to the maturity date. Daily Trades_i is a per bond metric and is equivalent to the total number of deals divided by the number of days on which the bond occurs in the sample. The time to maturity is the time in the number of years between the bond's settlement date and its maturity date. Age is the distance between the last two measures. Coupon rate relates to either a bond's coupon rate, zero-coupon rate or floating rate. The issued amount is the one of the bonds in millions of euros. Coupon Rate is the annual coupon rate.

For coupon bonds, Quoted Spread and Effective Spread display very equivalent outcomes. The links between them and the maturity of the bond are largely nonlinear. It is evident that, among the maturity group itself, outstanding and near-maturity bonds have the shortest bid-ask spreads, meanwhile those in their "mid-life" have upper spreads, revealing an upside-down U-shaped pattern.

The 5-min Single Proposals is the mean number of traders estimated at a frequency of 5 min and the Single Proposal Revisions is the frequency with which quotations vary. The findings show that the activity market is greater for longer maturity bonds. Market events have a convex association with time to expiration, reflecting the outcomes of the bid-ask spread, with a higher number of traders for bonds outstanding and near to expiration. The number of deals reflects positively on the number of dealers, while in a negative way on the number of price reviews.

2.6.2. *Time-series evidence*

We examine the characteristics of liquidity measures through time, and it relates to changes in credit. In particular, we study whether credit risk and liquidity estimates are correlated, and if convex or linear: i.e., that major movements in credit risk have a correspondingly greater effect than minor swings in the different liquidity measures. To explore this, we perform a regression of changing cash metrics on shifts in the CDS differential, its square and the amount transacted. Equation (50) details our regression model:

$$\Delta \mathrm{LM}_t = \beta_0 + \beta_1 \Delta \mathrm{CDS}_t + \beta_2 (\Delta \mathrm{CDS}_t)^2 + \beta_3 \mathrm{TradedQuantity}_t + \epsilon_t, \tag{50}$$

where $\Delta \mathrm{LM}_t$ is the measure of liquidity change from time $t-1$ to time t, $\Delta \mathrm{CDS}_t$ is the CDS change and $\mathrm{TradedQuantity}_t$ is the amount transacted in the market on that day.

The impact is meaningful as well, albeit with a smaller size, for the Effective Spread. The variation of the CDS differential and its square is highly correlated with the Amihud measure too. The amount detailed is adversely associated with the quoted and effective spread. Hence, it is probably caused by the degree of endogeneity of the decision to negotiate concerning the price differential. The quantity traded is as well favorably associated with Revisions per Single Proposal and with the Log Var, but adversely with the Total Quoted Quantity. So, when more knowledgeable dealers come into the market, the market developers are also less inclined to the contrarian way. Typically, a high traded quantity is linked to high price movements, resulting in that price volatility (Log Var) correlates positively with the quantity traded. Single 5-min proposals are related adversely to everyday commerce for zero-coupon bonds and favorably to coupon bonds.

3. Estimation Methods

3.1. *Convolutional neural network*

CNN is a kind of artificial neural network requiring a convolutional layer but may have additional layer types, including nonlinear, clustering and fully linked layers, that build a deep CNN (Albawi *et al.*, 2017; Wu, 2016; Stutz, 2014; Bouvrie, 2006). It can be beneficial, especially in the case of a CNN, depending on the application (Suryani *et al.*, 2016). Nevertheless, it provides further training parameters. In the CNN, convolutional filters are formed via the technique of backpropagation. The structure of the filter shapes differs according to the task at hand. For instance, in an application like face detection, one filter may undertake border removal, while another may perform eye extraction. But, we cannot

manage these filters in the CNN, and their assets are set by training (Albawi *et al.*, 2017; Hapke, 2016; Szegedy *et al.*, 2015; Zeiler and Fergus, 2014).

In the advection coating, the filters are slipped over the coating for the given incoming information. The sum of an item-by-item multiplying of the filters and the input responsive domain is then computed as the outcome of this layer. The loaded sum is positioned as the next layer's element (Wu, 2016; Stutz, 2014). Each convolutional operation is given by the fringe, the size of the filter and the zero packing. The fringe, being a solid positive integer, defines the step of the glide path. The filter size has to be stationary for all filters involved in the given convolutional operation. Zero padding inserts zero rows and zero columns into the source input matrix for managing the output feature map size (Guo *et al.*, 2016; Wu, 2016; O'Shea and Nash, 2015). Zero padding is primarily intended to fit the data on the edge of the input matrix. With no zero padding, the convolution outcome is lower than the input. Thus, the dimension of the network is reduced by making multiple convolution layers, limiting the number of convolutional layers in a network. Yet, zero-padding avoids network shrinkage and gives unbounded deep layers in our network configuration.

If nonlinearity is used, the main function is to adapt or short-circuit the output produced. Various nonlinear features can be used in CNNs. The rectified linear unit (ReLU), however, is among the commonly implemented nonlinearities in several areas, like image processing (Dumoulin and Visin, 2016; Wu, 2016). ReLU can be expressed as

$$\text{ReLU} = \begin{cases} 0, & \text{if } x < 0, \\ x, & \text{if } x \geq 0. \end{cases} \tag{51}$$

The pooling layer approximately narrows the size of the inputs. The most popular pooling method, max pooling, depicts the highest value within the pooling filter (2×2) as the output (Ba and Frey, 2013; Wan *et al.*, 2013). There are other pooling techniques, like averaging and summation. Nevertheless, max pooling is a very extended and powerful approach in the literature as it delivers meaningful findings by reducing the dimension of the input by 75% (Szegedy *et al.*, 2015; Han *et al.*, 2014).

The softmax layer is regarded as an ideal methodology for proving the categorical distribution. The softmax function, mainly employed in the output layer, is a standardized exponent of the output values (Peng *et al.*, 2017). This function is distinguishable and stands for a given likelihood of the output. In addition, the exponential element raises the probability of the maximum amount (Hapke, 2016). The equation softmax is as follows:

$$o_i = \frac{e^{z_i}}{\sum_{i=1}^{M} e^{z_i}}, \tag{52}$$

where o_i is the output softmax number i, z_i is the output i before the softmax and M is the number of total exit nodes.

3.2. *Recurrent convolutional neural network*

Recurrent neural networks (RNNs) have been implemented in various forecasting areas owing to their enormous forecasting efficiency. The prior computations performed are what form the output within the RNN structure (Wang *et al.*, 2017). For an entry sequence vector

x, the hidden nodes of a layer s, and the output of a shadow layer y, could be computed as shown in the following equations:

$$s_t = \sigma(W_{xs}x_t + W_{ss}s_{t-1} + b_s), \tag{53}$$

$$y_t = o(W_{so}s_t + b_y), \tag{54}$$

where W_{xs}, W_{ss} and W_{so} are the input layer weights x to the shadow layer s, by are the distortions of the shadow layer and the output layer. The following equation indicates that σ and o are the functions of activation.

$$\mathrm{STFT}\{z(t)\}(\tau,\omega) = \int_{-\infty}^{+\infty} z(t)\omega(t-\tau)e^{-j\omega t}dt), \tag{55}$$

where $z(t)$ is the oscillation signs, $\omega(t)$ is the Gaussian window function centered about 0. $T(\tau,\omega)$ is the function that expresses the vibration signs. To compute the convolutional operation hidden layers, the following equations are implemented:

$$S_t = \sigma(W_{TS} * T_t + W_{SS} * S_{t-1} + B_s), \tag{56}$$

$$Y_t = o(W_{YS} * S_t + B_y), \tag{57}$$

where W term shows the convolution kernels.

A RCNN can be stacked to set up a profound structure, named deep recurrent convolutional neural network (DRCNN) (Huang and Narayanan, 2017). To employ the DRCNN methodology in the task of prediction, the following equation defines the last stage of the network as a monitored machine learning layer:

$$\hat{r} = \sigma(W_h * h + b_h), \tag{58}$$

where W_h is the weight and b_h is the bias. The model estimates the residuals driven by the discrepancy of the planned and current findings in the trained phase (Ma and Mao, 2019). We apply stochastic gradient drop for the optimization to apprehend the benchmarks. Taking the data at time t to be r, the residual function is set as given in the following equation.

$$L(r,\hat{r}) = \frac{1}{2}\|r - \hat{r}\|_2^2. \tag{59}$$

3.3. *Long short-term memory*

LSTM is an improved RNN technology architecture that has become adapted to handle the time-dependent variables that occur in time series (Hochreiter and Schmidhuber, 1997). This kind of network provides the benefit of adding historical data to the forecasting of the variables' future state when the input data have several dependencies. In the RNN, the impact of recall is considered by employing an unwound cell loop that enables prior data to feed back into the following step prediction. Its structure, nevertheless, does not permit the processing of long-term dependencies efficiently, as its learning procedure causes gradients to disappear for back-propagation. To bridge this gap, LSTM networks have been built with an effective framework involving three doors: input gates, output gates and forgetting

gates that assure the conservation of the information prior to using a steady-state computation of the gradient. At all three gates within a cell state, data are handled by a sequential computation employing the next equations (Hochreiter and Schmidhuber, 1997; Vu *et al.*, 2020):

$$\begin{aligned} i_t &= \sigma(W_{ixt} + U_{iht-1} + b_i), \\ f_{t_w} &= \sigma(W_{fxt} + U_{fht-1} + b_f), \\ o_t &= \sigma(W_{oxt} + U_{oht} - 1 + b_o), \\ C_t &= \tanh(W_{cxt} + U_{cht-1} + b_c), \\ C_t &= f_{t_m} \otimes C_{t-1} + i_t \otimes C_t, \\ h_t &= o_t \otimes \tanh(Ct), \end{aligned}$$

where xt nominates the input variable at the current time step, ht is the exit of the prior cell, $Ct-1$ is the preceding cell state giving the past data. These settings are employed with a sample of the weight matrices and bias vectors in the logistic sigmoid σ, and tanh functions at the input, forget and outputs gates.

Concerning the option of the best network structure of LSTM networks to get precise forecasts, a unique hidden layer is embraced where the number of nodes is set on conforming to the next law:

$$(n_{\text{in}} + 1) \times n_{\text{hid}} + (n_{\text{hid}} + 1) \times n_{\text{out}} \leq 1/\alpha \times n_{\text{train}},$$

whereas n_{in} indicates the number of nodes in the input layer, n_{out} is the number of nodes in the output layer, n_{hid} is the number of nodes in the hidden layer, n_{train} is the number of training data and α is a coefficient, which changes from 1 to over 10. In this investigation, to keep away from overfitting, α is given a value greater than 2 as the training data double degrees of liberty in the process of formation.

4. Sample, Data and Variables

Market data for long-term bonds with maturities of 2, 5, 10 and 30 years and short-term treasury bills with maturities of 1, 3 and 6 months have been used for the cases of Greece and Thailand. The speculative pressure scenarios are generated from the modeling expressed in Section 2, concerning the scenarios. Macroeconomic information for the models used was obtained from International Monetary Fund, World Bank and Eurostat statistics. The bond market data used were extracted from the Eikon database of Refinitiv (Thomson Reuters). The period chosen was from 2002Q1 to 2021Q2.

Empirical research for forecasting these models of market microstructure has completed the following five steps: creating a sample, data preprocessing, construction of model into the neural networks method, accuracy assessment, and classification and forecasting. Regarding the point of creating a sample is based on getting the data from relevant sources, as in our case with Eikon database from Thomson Reuters. The step data preprocessing consists of the discretization of attributes of continuous values, generalization of data and analysis of attribute relativity, and elimination of outliers. For its part, the market microstructure and speculative attacks models proposed in this study have been estimated, thanks

to these models are in linearized, and hence, it is possible to introduce every variable no making transformations. To do this, and randomly, the sample is divided into two sets of mutually exclusive data: training (or in-sample) data set (70%), and testing (or out-sample) data set (30%). During the estimations of results, the cross-validation method with 10-fold and 500 iterations has been applied to obtain error ratios (Salas *et al.*, 2020). The first data set is used for model training, that is, for parameter estimation. Finally, the second data set (testing) is used to evaluate the prediction accuracy of the model during the accuracy assessment step. In an additional way, the differences between observed and predicted values examine the robustness of the every neural networks method and its ability to predict both the trend in government bond markets and the possible speculative attack scenario as well.

5. Results

In the case of Greece, Figures 1–3 show the level of accuracy in training data in CNN, RCNN and LSTM methods, respectively. These results also appear in Annex A. Table 1 displays the results of Precision Testing, applied to assess the built model and make predictions. Tables 2 and 3 exhibit the RMSE and the MAPE. In all six models, the level of accuracy exceeds in every moment 89.99% in short-term maturity and 88.74% in long-term for the training results. According to the testing results, the precision level overcomes at all times, 87.40% in short-term maturity and 86.19% in long-term. The model with the highest level of accuracy in all three methods is that of TWBAS with an accuracy over 95.15% and 92.42% in short term for training and test results, respectively, and the percentages of 93.83% and 91.14% in long term for in-sample and out-sample results accordingly, followed by the volatility model with an average precision of 93.03% and 91.74% in short term and long term for each of them for the training results. In the case of the testing results in the volatility model, the average accuracy rates are 90.36% and 89.11% in short term and long term separately. Besides, RMSE and MAPE levels are adequate. All models in all three methods have low RMSE values, being in a range of 0.10–0.21. The MAPE values, the result of measuring the size of the absolute error in percentage terms, are acceptable for all the models constructed too. On the other hand, the

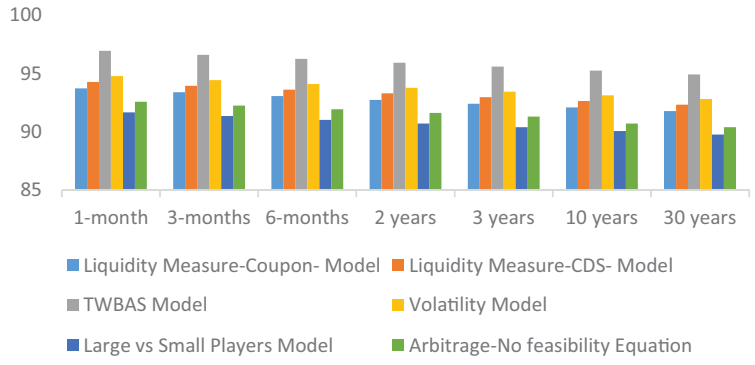

Figure 1. Results of Precision Training in CNN Method (%): Greece

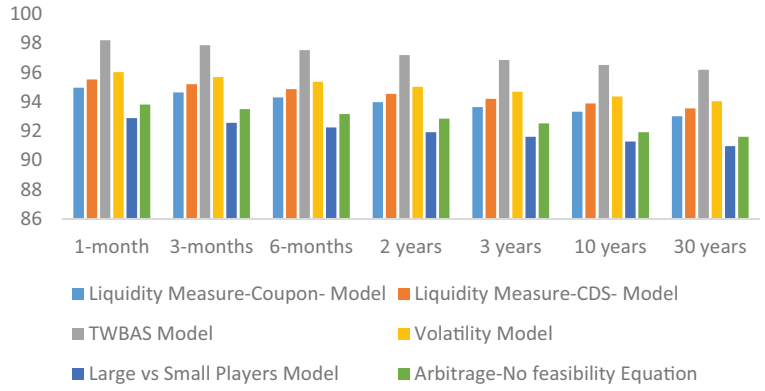

Figure 2. Results of Precision Training in RCNN Method (%): Greece

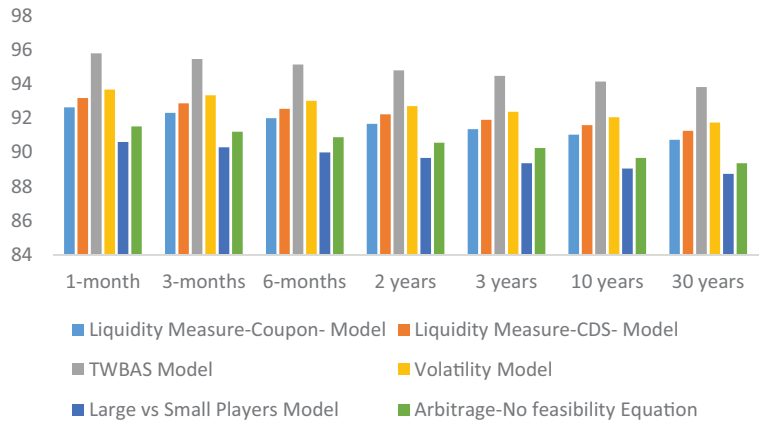

Figure 3. Results of Precision Training in LSTM Method (%): Greece

method that best adjusts the result in terms of residuals is RCNN with 97.52% (training) and 94.72% (testing) accuracy in short term and 96.17% (training) and 93.41% (testing) in long term, followed by CNN with 96.25% and 94.92% for training results in short and long maturity, respectively. For the testing results, the precision is 93.49% and 92.19% in short and long maturity individually. The accuracy levels tend to decrease slightly with longer maturities. Thus, in the TBWAS model of the RCNN method, the accuracy when the maturity is 1 month reaches 98.20% (training) and 95.38% (testing), decreasing to 96.17% (training) and 93.41% (testing) when the maturity is extended to 30 years.

For Thailand, Figures 4–6 display the accuracy level on the training data in the CNN, RCNN and LSTM methods correspondingly, which is also listed in Annex B. Table 4 displays the findings of testing precision, and Tables 5 and 6 report the RMSE and the MAPE. In the six models in the three methods, the accuracy level for training data always exceeds 87.87% at maturity in the short term and 86.66% in long term, and the precision level for testing data all the time outperforms 85.34% in short-term maturity and 84.16% in long term. The results are slightly worse than in Greece, but the order of accuracy is the

Table 1. Results of Precision Testing (%): Greece

	Liquidity Measure Coupon Model	Liquidity Measure CDS Model	TWBAS Model	Volatility Model	Large versus Small Players Model	Arbitrage-No Feasibility Equation
			CNN			
1 Month	91.02	91.57	94.14	92.04	89.03	89.92
3 Months	90.71	91.25	93.81	91.72	88.72	89.61
6 Months	90.39	90.93	93.49	91.40	88.41	89.30
2 Years	90.08	90.61	93.16	91.09	88.11	88.99
3 Years	89.76	90.30	92.84	90.77	87.80	88.68
10 Years	89.45	89.99	92.52	90.45	87.50	88.11
30 Years	89.14	89.67	92.19	90.14	87.19	87.80
			RCNN			
1 Month	92.22	92.77	95.38	93.25	90.20	91.11
3 Months	91.90	92.45	95.05	92.93	89.89	90.79
6 Months	91.58	92.13	94.72	92.61	89.58	90.47
2 Years	91.26	91.81	94.39	92.28	89.26	90.16
3 Years	90.94	91.49	94.06	91.96	88.95	89.85
10 Years	90.63	91.17	93.73	91.64	88.65	89.27
30 Years	90.31	90.85	93.41	91.32	88.34	88.96
			LSTM			
1 Month	89.98	90.52	93.06	90.99	88.01	88.89
3 Months	89.67	90.20	92.74	90.67	87.70	88.59
6 Months	89.35	89.89	92.42	90.36	87.4	88.28
2 Years	89.04	89.58	92.09	90.04	87.1	87.97
3 Years	88.74	89.27	91.77	89.73	86.79	87.67
10 Years	88.43	88.96	91.46	89.42	86.49	87.10
30 Years	88.12	88.65	91.14	89.11	86.19	86.79

same, as the best methodology is RCNN with 95.23% and 92.49% in short-term maturity for training and testing results, respectively, and 93.91% and 91.21% in long term, in training and testing data accordingly, followed by CNN with 91.29% and 90.02% in short and long terms, respectively, for testing results, and in case of training results 93.99% and 92.69% in the short and long terms separately. Like in the example of Greece, it is once again the model TWBAS, the one that has the greatest level of precision. For its part, the RMSE and MAPE levels are suitable. As in the previous case, the precision values are slightly lower with longer-term maturities. Hence, in the RCNN TBWAS model, the precision at 1-month maturity stands at 95.89% (training) and 93.13% (testing), decreasing to 93.91% (training) and 91.21% (testing) when the maturity is prolonged to 30 years.

Table 2. Results of Accuracy Evaluation: RMSE (Root Mean Squared Error): Greece

	Liquidity Measure Coupon Model	Liquidity Measure CDS Model	TWBAS Model	Volatility Model	Large versus Small Players Model	Arbitrage-No Feasibility Equation
			CNN			
1 Month	0.10	0.10	0.10	0.10	0.10	0.10
3 Months	0.11	0.11	0.11	0.11	0.11	0.11
6 Months	0.12	0.12	0.13	0.12	0.12	0.12
2 Years	0.13	0.13	0.14	0.13	0.13	0.13
3 Years	0.14	0.15	0.15	0.15	0.14	0.14
10 Years	0.16	0.16	0.16	0.16	0.15	0.16
30 Years	0.17	0.17	0.18	0.18	0.17	0.17
			RCNN			
1 Month	0.10	0.10	0.11	0.10	0.10	0.10
3 Months	0.11	0.11	0.12	0.11	0.11	0.11
6 Months	0.12	0.12	0.13	0.12	0.12	0.12
2 Years	0.13	0.14	0.14	0.14	0.13	0.13
3 Years	0.15	0.15	0.15	0.15	0.14	0.14
10 Years	0.16	0.16	0.17	0.16	0.16	0.16
30 Years	0.18	0.18	0.18	0.18	0.17	0.17
			LSTM			
1 Month	0.12	0.12	0.12	0.12	0.11	0.12
3 Months	0.13	0.13	0.13	0.13	0.13	0.13
6 Months	0.14	0.14	0.15	0.14	0.14	0.14
2 Years	0.15	0.15	0.16	0.16	0.15	0.15
3 Years	0.17	0.17	0.17	0.17	0.16	0.17
10 Years	0.18	0.18	0.19	0.19	0.18	0.18
30 Years	0.20	0.20	0.21	0.20	0.20	0.20

Emerging markets experience a loss of foreign exchange access to international capital markets when currency and banking crises occur. Moreover, due to the prevalent reliance on short-term debt financing, the public and private sectors in these economies often have to repay their outstanding debts in the short term. A slowdown in capital inflows or their reversal could lead the country to insolvency or sharply reduce the productivity of its existing capital stock (Calvo and Reinhart, 2000). International capital markets are, therefore, volatile, both downward and upward, with emerging market economies suffering the most. The Asian financial crisis of 1997 revealed the region's vulnerability to cross-border capital flows. During this crisis, for instance, large currency depreciation and falling equity prices in Thailand led international institutional investors to suffer large capital losses. Such losses incurred may have driven investors to sell securities in other emerging

Table 3. Results of Accuracy Evaluation: MAPE: Greece

	Liquidity Measure Coupon Model	Liquidity Measure CDS Model	TWBAS Model	Volatility Model	Large versus Small Players Model	Arbitrage-No Feasibility Equation
			CNN			
1 Month	0.44	0.44	0.45	0.44	0.43	0.43
3 Months	0.48	0.48	0.49	0.48	0.47	0.47
6 Months	0.52	0.53	0.54	0.53	0.51	0.52
2 Years	0.57	0.57	0.59	0.58	0.56	0.56
3 Years	0.62	0.63	0.65	0.63	0.61	0.62
10 Years	0.68	0.69	0.71	0.69	0.67	0.67
30 Years	0.75	0.75	0.77	0.76	0.73	0.74
			RCNN			
1 Month	0.44	0.45	0.46	0.45	0.43	0.44
3 Months	0.48	0.49	0.50	0.49	0.47	0.48
6 Months	0.53	0.53	0.55	0.54	0.52	0.52
2 Years	0.58	0.58	0.59	0.59	0.57	0.57
3 Years	0.63	0.64	0.65	0.64	0.62	0.62
10 Years	0.69	0.69	0.72	0.70	0.68	0.68
30 Years	0.76	0.76	0.78	0.77	0.74	0.75
			LSTM			
1 Month	0.51	0.51	0.52	0.51	0.49	0.50
3 Months	0.55	0.56	0.57	0.56	0.54	0.55
6 Months	0.60	0.61	0.62	0.61	0.59	0.59
2 Years	0.66	0.67	0.68	0.67	0.65	0.65
3 Years	0.72	0.73	0.75	0.73	0.71	0.71
10 Years	0.79	0.79	0.82	0.8	0.77	0.78
30 Years	0.86	0.87	0.89	0.87	0.84	0.85

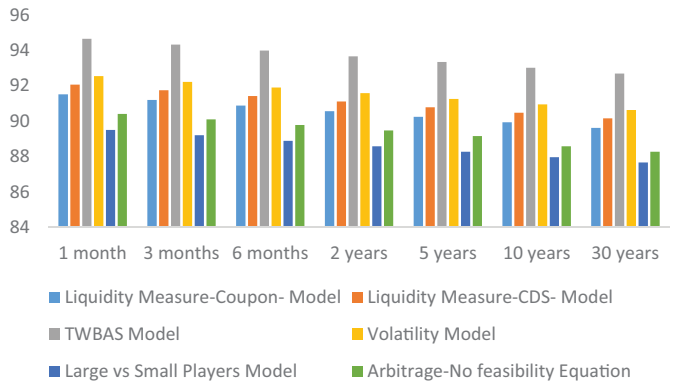

Figure 4. Results of Precision Training in CNN Method (%): Thailand

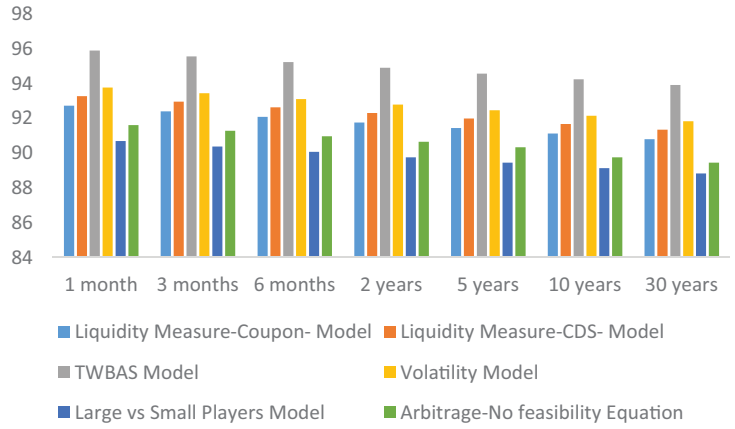

Figure 5. Results of Precision Training in RCNN Method (%): Thailand

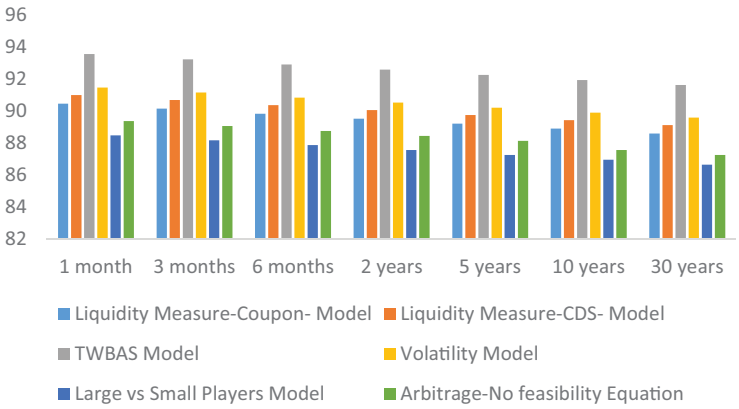

Figure 6. Results of Precision Training in LSTM Method (%): Thailand

economies to get cash in anticipation of a greater redemption frequency. Commercial banks that concentrate their lending in certain regions may also face liquidity problems (Dornbusch *et al.*, 2000). Zhang (2001) concluded that the probability of a currency being attacked in one period is influenced by the frequency of speculative attacks in other countries before that period, due to the contagion effect. The reason for the attacks at the beginning remains an enigma, but the dynamics of regional duration seem to explain the evolution of the 1997 Asian crisis in Thailand quite well. This crisis resulted in a constraint on the ability of Thai firms to undertake FDI, extend credit and so on. The Thai government increased public debt to rescue the banks or the business sector. So, there was a fiscal consolidation at some point, and then they reinforced the regulatory framework for the financial and monetary sector, which helped them to allow the exchange rate to be more flexible (Charoenseang and Manakit, 2002).

In the case of Greece, most of the attention on the Greek crisis has focused on the acute problems of financing the Greek debt and initiating the required Greek fiscal reduction strategy. The sovereign debt crisis in Greece in 2010 created serious problems in the

Table 4. Results of Precision Testing (%): Thailand

	Liquidity Measure Coupon Model	Liquidity Measure CDS Model	TWBAS Model	Volatility Model	Large versus Small Players Model	Arbitrage-No Feasibility Equation
			CNN			
1 Month	88.88	89.41	91.92	89.88	86.94	87.81
3 Months	88.57	89.1	91.6	89.56	86.63	87.5
6 Months	88.26	88.79	91.29	89.25	86.33	87.2
2 Years	87.96	88.48	90.97	88.94	86.03	86.9
5 Years	87.65	88.17	90.65	88.63	85.73	86.59
10 Years	87.35	87.87	90.34	88.33	85.44	86.03
30 Years	87.04	87.56	90.02	88.02	85.14	85.73
			RCNN			
1 Month	90.05	90.59	93.13	91.06	88.08	88.96
3 Months	89.74	90.27	92.81	90.74	87.77	88.65
6 Months	89.42	89.96	92.49	90.43	87.47	88.35
2 Years	89.11	89.65	92.17	90.11	87.16	88.04
5 Years	88.80	89.33	91.85	89.80	86.86	87.73
10 Years	88.49	89.02	91.53	89.49	86.56	87.16
30 Years	88.19	88.71	91.21	89.18	86.26	86.86
			LSTM			
1 Month	87.86	88.39	90.87	88.85	85.94	86.80
3 Months	87.56	88.08	90.56	88.54	85.64	86.50
6 Months	87.25	87.77	90.24	88.23	85.34	86.20
2 Years	86.95	87.47	89.93	87.92	85.05	85.90
5 Years	86.65	87.16	89.61	87.62	84.75	85.60
10 Years	86.35	86.86	89.30	87.31	84.46	85.05
30 Years	86.05	86.56	88.99	87.01	84.16	84.75

financial markets and came close to provoking the breakdown of the euro, mainly due to speculative attacks (Wihlborg *et al.*, 2010). Specifically, Greece's government had amassed huge debts, faced falling tax revenues from the recession, confronted nonsustainable interest rates in bond markets and was on the verge of insolvency. Up to now, this situation has been handled by European leaders using a mix of additional rescue loans, debt renegotiations and "haircuts" as well as severe austerity measures for the Greek government (Seyler and Levendis, 2015).

On balance, in both countries, the method with the highest precision is RCNN, being the models TWBAS and volatility the most accurate. TWBAS provides robustness since it does not rely on strike prices, which are utilized for all other liquidity metrics. In previous literature, some authors have used TWBAS and volatility models to measure the liquidity

Table 5. Results of Accuracy Evaluation: RMSE (Root Mean Squared Error): Thailand

	Liquidity Measure Coupon Model	Liquidity Measure CDS Model	TWBAS Model	Volatility Model	Large versus Small Players Model	Arbitrage-No Feasibility Equation
			CNN			
1 Month	0.22	0.22	0.23	0.22	0.21	0.22
3 Months	0.24	0.24	0.25	0.24	0.23	0.24
6 Months	0.26	0.26	0.27	0.26	0.26	0.26
2 Years	0.29	0.29	0.30	0.29	0.28	0.28
5 Years	0.31	0.32	0.32	0.32	0.31	0.31
10 Years	0.34	0.35	0.36	0.35	0.34	0.34
30 Years	0.38	0.38	0.39	0.38	0.37	0.37
			RCNN			
1 Month	0.22	0.22	0.23	0.22	0.22	0.22
3 Months	0.24	0.24	0.25	0.24	0.24	0.24
6 Months	0.27	0.27	0.27	0.27	0.26	0.26
2 Years	0.29	0.29	0.30	0.29	0.28	0.29
5 Years	0.32	0.32	0.33	0.32	0.31	0.31
10 Years	0.35	0.35	0.36	0.35	0.34	0.34
30 Years	0.38	0.38	0.39	0.39	0.37	0.38
			LSTM			
1 Month	0.25	0.25	0.26	0.26	0.25	0.25
3 Months	0.28	0.28	0.29	0.28	0.27	0.27
6 Months	0.30	0.31	0.31	0.31	0.30	0.30
2 Years	0.33	0.33	0.34	0.34	0.33	0.33
5 Years	0.36	0.37	0.38	0.37	0.36	0.36
10 Years	0.40	0.40	0.41	0.40	0.39	0.39
30 Years	0.44	0.44	0.45	0.44	0.43	0.43

of government bonds in the euro zone, including Greece (Darbha and Dufour, 2013; Pelizzon *et al.*, 2013; Ehrmann and Fratzscher, 2017; Benos *et al.*, 2019), and in Asian countries, especially in Thailand (Piesse *et al.*, 2007; Chabchitrchaidol and Panyanukul, 2008; Pholphirul, 2009; Bai *et al.*, 2013; Yurastika and Wibowo, 2021). Darbha and Dufour (2013) and Pelizzon *et al.* (2013) found that more recently issued and larger bonds have lower Quoted Bid-Ask Spreads. They concluded that the lower the bid-ask spread, the higher the liquidity. For its part, Pholphirul (2009) showed that the investment growth in Thailand is more significantly determined by its volatility than by consumption or production. Nevertheless, concerning the methodology employed by these authors, they have focused exclusively on statistical and econometric methods, such as Ordinary Least Squares, autoregression and generalized autoregressive conditional heteroskedasticity

Table 6. Results of Accuracy Evaluation: MAPE: Thailand

	Liquidity Measure Coupon Model	Liquidity Measure CDS Model	TWBAS Model	Volatility Model	Large versus Small Players Model	Arbitrage-No Feasibility Equation
			CNN			
1 Month	0.56	0.56	0.58	0.56	0.54	0.55
3 Months	0.61	0.61	0.63	0.62	0.60	0.60
6 Months	0.67	0.67	0.69	0.67	0.65	0.66
2 Years	0.73	0.73	0.75	0.74	0.71	0.72
5 Years	0.80	0.81	0.82	0.81	0.78	0.79
10 Years	0.87	0.88	0.90	0.88	0.85	0.86
30 Years	0.95	0.96	0.99	0.97	0.93	0.94
			RCNN			
1 Month	0.50	0.57	0.58	0.57	0.55	0.56
3 Months	0.62	0.62	0.64	0.62	0.60	0.61
6 Months	0.67	0.68	0.70	0.68	0.66	0.67
2 Years	0.74	0.74	0.76	0.75	0.72	0.73
5 Years	0.81	0.81	0.84	0.82	0.79	0.80
10 Years	0.88	0.89	0.91	0.89	0.86	0.87
30 Years	0.97	0.97	1.00	0.98	0.95	0.96
			LSTM			
1 Month	0.64	0.65	0.67	0.65	0.63	0.64
3 Months	0.71	0.71	0.73	0.71	0.69	0.70
6 Months	0.77	0.78	0.80	0.78	0.75	0.76
2 Years	0.84	0.85	0.87	0.85	0.83	0.83
5 Years	0.92	0.93	0.96	0.93	0.90	0.91
10 Years	1.01	1.02	1.05	1.02	0.99	1.00
30 Years	1.11	1.11	1.14	1.12	1.08	1.09

(GARCH), having higher error levels results than those achieved in our research. For instance, the work of Ehrmann and Fratzscher (2017) gets RMSE values close to 0.62, the study of Benos *et al.* (2019) gets around 0.60, in the work of Bai *et al.* (2013) it approaches 0.55 and in the case of Yurastika and Wibowo (2021) it approached 0.50. So, taken as a whole, our results provide a much higher probability of prediction than previous studies, and the difference presented by the computational methodologies used in this investigation far surpassed the precision revealed by the prior literature. Table 7 places our research among comparable research in predicting speculative attacks in government bonds.

These results exhibit the higher firmness suggested by the RCNN method compared to the others, mainly considering the RMSE results achieved by the statistical methods. This ensemble of computational methodologies, found to be very precise, is a novel group of

Table 7. Comparison Between This Research and Other Research

	Year	Algorithm Used	Countries	Result (RMSE)
This research	2022	Machine Learning	Greece and Thailand	0.18–0.39
Yurastika and Wibowo	2021	GARCH	Indonesia, Malaysia, Philippines, Singapore and Thailand	0.50
Benos *et al.*	2019	Autoregression	USA	0.60
Ehrmann and Fratzscher	2017	GARCH	Euro Area	0.62
Bai *et al.*	2013	Autoregression	China	0.55

methodologies that evaluate speculative attacks and, hence, differs from those reported in the prior literature. The main advantage of deep neural network methods over classical statistical/econometric methods is that machine learning algorithms could manage a huge quantity of both unstructured and structured data and make decisions or predictions quickly. This enhanced output is achieved because machine learning models do not create any predetermined suppositions regarding the functional form of the equation, the interplay in the middle of the variables, and the parameters' statistical distribution. Machine learning methods, on the other side, concentrate on precise forecastings for certain output variables in the light of several other variables (Ghoddusi *et al.*, 2019).

6. Conclusions

This study has developed a new machine learning estimation for market microstructure and speculative attack models to prove his accuracy in market microstructure models and that this mechanism of speculative attack could happen in the government bond market too. The methodology applied is deep neural networks techniques using data for long-term bonds with maturities of 2, 5, 10 and 30 years and short-term treasury bills with maturities of 1, 3 and 6 months for the cases of Greece and Thailand in the time 2004Q1-2020Q4. Three different Neural Network methods in the estimation of six market microstructure and speculative attacks models (liquidity measure coupon, liquidity measure CDS, TWBAS, volatility, large versus small players and arbitrage no feasibility equation) have been constructed to achieve a robust accuracy capacity, such as CNN, RCNN and LSTM. The methodology that has achieved the greatest levels of precision is RCNN. Most methodologies have exhibited a very low error rate and stability of estimates from speculative attack models, making them an attractive alternative to traditional statistical methods.

We demonstrate that RCNN method identifies and quantifies financial market risks in a proactive approach and is a reliable solution to deal with the uncertainty and complexity of the financial system arising from speculative attacks, providing more information on the possible events that may occur in the government bond market. Besides, our results achieve a high level of accuracy, in a range of 94.72%–93.41% in short-term and long-term maturity in the case of Greece, and 92.49%–91.21% in Thailand.

Our model guides policymakers and empiricists who assess the effectiveness of market designs. So, our findings are relevant for financial organizations and policymakers, who should understand how the bond market functions to design the regulation of this system and to identify possible systemic risks. In addition, our study may be useful for market regulators (national central banks) to deal with transparency issues in relation the organization of treasury bond markets and appropriate revelation of data and to assess the behavior of single traders.

In conclusion, this study offers an excellent contribution to the research on the sovereign bond market, as the results achieved have significant implications for the decisions of public and financial institutions in the future, allowing them to avoid liquidity risks by anticipating possible speculative attacks in the bond market. Further research could apply these Neural Network methods in models of other financial assets to check their estimation accuracy in the face of any asset pricing challenge, as it can represent a great starting point for modeling and estimating new strategies and models on speculation scenarios that accurately anticipate risk situations for financial stability, as is the recent case of cryptocurrencies.

Annex A. Results of Precision Training (%): Greece

Table A.1.

	Liquidity Measure Coupon Model	Liquidity Measure CDS Model	TWBAS Model	Volatility Model	Large versus Small Players Model	Arbitrage-No Feasibility Equation
			CNN			
1 Month	93.72	94.28	96.93	94.77	91.67	92.59
3 Months	93.39	93.95	96.59	94.44	91.35	92.26
6 Months	93.06	93.62	96.25	94.11	91.03	91.94
2 Years	92.74	93.30	95.92	93.78	90.71	91.62
3 Years	92.42	92.97	95.59	93.45	90.40	91.31
10 Years	92.10	92.65	95.25	93.13	90.08	90.71
30 Years	91.78	92.33	94.92	92.81	89.77	90.40
			RCNN			
1 Month	94.95	95.51	98.20	96.01	92.87	93.80
3 Months	94.62	95.18	97.86	95.68	92.55	93.48
6 Months	94.29	94.85	97.52	95.35	92.23	93.15
2 Years	93.96	94.52	97.18	95.01	91.91	92.83
3 Years	93.63	94.19	96.84	94.68	91.59	92.51
10 Years	93.31	93.87	96.51	94.35	91.27	91.91
30 Years	92.99	93.54	96.17	94.03	90.95	91.59

Table A.1. (*Continued*)

	Liquidity Measure Coupon Model	Liquidity Measure CDS Model	TWBAS Model	Volatility Model	Large versus Small Players Model	Arbitrage-No Feasibility Equation
			LSTM			
1 Month	92.64	93.19	95.81	93.68	90.61	91.52
3 Months	92.32	92.87	95.48	93.35	90.30	91.21
6 Months	92.00	92.55	95.15	93.03	89.99	90.89
2 Years	91.68	92.23	94.82	92.71	89.67	90.57
3 Years	91.36	91.91	94.49	92.38	89.36	90.26
10 Years	91.04	91.59	94.16	92.06	89.05	89.67
30 Years	90.73	91.27	93.83	91.74	88.74	89.36

Annex B. Results of Precision Training (%): Thailand

Table B.1.

	Liquidity Measure Coupon Model	Liquidity Measure CDS Model	TWBAS Model	Volatility Model	Large versus Small Players Model	Arbitrage-No Feasibility Equation
			CNN			
1 Month	91.51	92.06	94.65	92.54	89.51	90.41
3 Months	91.20	91.74	94.32	92.22	89.20	90.10
6 Months	90.88	91.42	93.99	91.90	88.89	89.78
2 Years	90.56	91.11	93.67	91.58	88.58	89.47
5 Years	90.25	90.79	93.34	91.26	88.28	89.16
10 Years	89.94	90.47	93.02	90.94	87.97	88.58
30 Years	89.62	90.16	92.69	90.63	87.66	88.28
			RCNN			
1 Month	92.72	93.27	95.89	93.76	90.69	91.60
3 Months	92.40	92.95	95.56	93.43	90.37	91.28
6 Months	92.07	92.62	95.23	93.11	90.06	90.96
2 Years	91.75	92.30	94.90	92.78	89.75	90.65
5 Years	91.44	91.98	94.57	92.46	89.44	90.33
10 Years	91.12	91.66	94.24	92.14	89.13	89.75
30 Years	90.80	91.34	93.91	91.82	88.82	89.44

Table B.1. (*Continued*)

	Liquidity Measure Coupon Model	Liquidity Measure CDS Model	TWBAS Model	Volatility Model	Large versus Small Players Model	Arbitrage-No Feasibility Equation
			LSTM			
1 Month	90.47	91.01	93.56	91.48	88.49	89.38
3 Months	90.15	90.69	93.24	91.16	88.18	89.06
6 Months	89.84	90.38	92.92	90.84	87.87	88.76
2 Years	89.53	90.06	92.59	90.53	87.57	88.45
5 Years	89.22	89.75	92.27	90.21	87.26	88.14
10 Years	88.91	89.44	91.95	89.90	86.96	87.57
30 Years	88.60	89.13	91.63	89.59	86.66	87.26

References

Adler, RL and TJ Rivlin (1964). Ergodic and mixing properties of Chebyshev polynomials. *Proceedings of the American Mathematical Society*, 15, 794.

Albawi, S, T Mohammed and S Al-azawi (2017). Understanding of a convolutional neural network. In *Proc. 2017 Int. Conf. Engineering & Technology (ICET'2017)*, pp. 274–279. Antalya, Turkey: Akdeniz University.

Armstrong, JS (1985). *Long-Range Forecasting: From Crystal Ball to Computer.* 2nd Edition. Hoboken, NJ: Wiley.

Ba, J and B Frey (2013). Adaptive dropout for training deep neural networks. In *Proc. Advances in Neural Information Processing Systems*, pp. 3084–3092. MIT Press: Lake Tahoe, NV.

Back, K, R Liu and A Teguia (2019). Signaling in OTC markets: Benefits and costs of transparency. *Journal of Financial and Quantitative Analysis*, 55(1), 47–75.

Bai, J, M Fleming and C Horan (2013). The microstructure of China's government bond market, Staff Report, No. 622, Federal Reserve Bank of New York, New York, NY.

Bao, J, J Pan and J Wang (2011). The illiquidity of corporate bonds. *Journal of Finance*, 66(3), 911–946.

Beber, A, MW Brandt and KA Kavajecz (2009). Flight-to-quality or flight-to-liquidity? Evidence from the Euro-Area bond market. *Review of Financial Studies*, 22(3), 925–957.

Benchimol, J, and A Fourçans (2017). Money and monetary policy in the Eurozone: An empirical analysis during crises. *Macroeconomic Dynamics*, 21, 677–707.

Benos, E, R Payne and M Vasios (2019). Centralized trading, transparency, and interest rate swap market liquidity: Evidence from the implementation of the Dodd–Frank act. *Journal of Financial and Quantitative Analysis*, 55(1), 159–192.

Bergh, A and M Karlsson (2010). Government size and growth: Accounting for economic freedom and globalization. *Public Choice*, 142, 195–213.

Bertola, G and RJ Caballero (1992). Target zones and realignments. *American Economic Review*, 82, 520–536.

Bessembinder, H, C Spatt and K Venkataraman (2020). A survey of microstructure of fixed-income market. *Journal of Financial and Quantitative Analysis*, 55(1), 1–45. doi:10.1017/S0022109019000231.

Biais, B and R Green (2019). The microstructure of the bond market in the 20th century. *Review of Economic Dynamics*, 33, 250–271.

Bouvrie, J (2006). Notes on convolutional neural networks. *Cogprints*. http://cogprints.org/5869/.
Calvo, GA and CM Reinhart (2000). Consequences and policy options. In *Reforming the International Monetary and Financial System*, Vol. 175.
Carfì, D and F Lanzafame (2013). A quantitative model of speculative attack: Game complete analysis and possible normative defenses. In *Financial Markets: Recent Developments, Emerging Practices and Future Prospects*, Chapter 9, M Bahmani-Oskooee and S Bahmani (eds.). Nova Science. https://www.novapublishers.com/catalog/product_info.php?products_id=46483.
Chabchitrchaidol, A and S Panyanukul (2008). *Key Determinants of Liquidity in the Thai Bond Market.* Bank of Thailand: Bangkok, Thailand.
Charoenseang, J and P Manakit (2002). Financial crisis and restructuring in Thailand. *Journal of Asian Economics*, 13(5), 597–613.
Corsetti, G, A Dasgupta, S Morris and HS Shin (2004). Does one Soros make a difference? A theory of currency crises with large and small traders. *Review of Economic Studies*, 71(1), 87–114.
Corsetti, G, K Kuester, A Meier and GJ Müller (2014). Sovereign risk and belief-driven fluctuations in the euro area. *Journal of Monetary Economics*, 61, 53–73.
Darbha, M and A Dufour (2012). Measuring Euro area government bond market liquidity and its asset pricing implications, Working Paper, University of Reading.
Darbha, M and A Dufour (2013). Microstructure of the Euro-area government bond market. In *Market Microstructure in Emerging and Developed Markets*, Robert W. Kolb Series in Finance, HK Baker and H Kiymaz (eds.). Wiley: Hoboken, NJ, USA.
De Grauwe, P and Y Ji (2012). Mispricing of sovereign risk and macroeconomic stability in the Eurozone. *Journal of Common Market Studies*, 50, 866–880.
De Grauwe, P and Y Ji (2013). Self-fulfilling crises in the Eurozone: An empirical test. *Journal of International Money and Finance - European Sovereign Debt Crisis: Background & Perspective*, 34, 15–36.
De Grauwe, P (2012). The governance of a fragile Eurozone. *Australian Economic Review*, 45, 255–268.
Della Posta, P (2016). Currency and external debt crises: A unifying framework. *Journal of Policy Modeling*, 38, 723–736.
Della Posta, P (2016). Self-fulfilling and fundamentals based speculative attacks: A theoretical interpretation of the euro area crisis. *Global Economy Journal*, 16, 459–478.
Della Posta, P (2021). Government size and speculative attacks on public debt. *International Review of Economics & Finance*, 72(C), 79–89.
Dornbusch, R, YC Park and S Claessens (2000). Contagion: How it spreads and how it can be stopped. *World Bank Research Observer*, 15(2), 177–197.
Dufour, A and M Nguyen (2012). Permanent trading impacts and bond yields. *The European Journal of Finance*, 18(9), 841–864.
Dumoulin, V and F Visin (2016). A guide to convolution arithmetic for deep learning. http://arxiv.org/abs/1603.07285.
Ehrmann, M and M Fratzscher (2017). Euro area government bonds–Fragmentation and contagion during the sovereign debt crisis. *Journal of International Money and Finance*, 70, 26–44.
Fleming, MJ, B Mizrach and G Nguyen (2018). The microstructure of a US Treasury ECN: The BrokerTec platform. *Journal of Financial Markets*, 40, 2–22.
Fleming, MJ (2003). Measuring treasury market liquidity. *Federal Reserve Bank of New York Economic Policy Review*, 9(3), 83–108.
Frömmel, M, X Han and S Kratochvil (2014). Modeling the daily electricity price volatility with realized measures. *Energy Economics*, 44, 492–502.
Friewald, N and F Nagler (2019). Over-the-counter market frictions and yield spread changes. *Journal of Finance*, 74(6), 3217–3257.

Fujimoto, J (2014). Speculative attacks with multiple targets. *Economic Theory*, 57, 89–132.
Ghoddusi, H, GG Creamer and N Rafizadeh (2019). Machine learning in energy economics and finance: A review. *Energy Economics*, 81, 709–727.
Glode, V and C Opp (2020). Over-the-counter vs. limit-order markets: The role of traders' expertise. *Review of Financial Studies*, 33(2), 866–915.
Goyenko, R, A Subrahmanyam and A Ukhov (2011). The term structure of bond market liquidity and its implications for expected bond returns. *Journal of Financial and Quantitative Analysis*, 46, 1.
Guo, Y, Y Liu, A Oerlemans, S Lao, S Wu and MS Lew (2016). Deep learning for visual understanding: A review. *Neurocomputing*, 187, 27–48.
Han, K, D Yu and I Tashev (2014). Speech emotion recognition using deep neural network and extreme learning machine. In *Proc. Fifteenth Annual Conf. Int. Speech Communication Association*, Singapore.
Hapke, H (2016). Introduction to convolutional neural networks. https://www.slideshare.net/hanneshapke/introduction-to-convolutional-neural-networks.
Haugom, E and CJ Ullrich (2012). Forecasting spot price volatility using the short-term forward curve. *Energy Economics*, 34(6), 1826–1833.
Hochreiter, S and J Schmidhuber (1997). Long short-term memory. *Neural Computation*, 9(8), 1735–1780.
Horváth, D, M Gmitra and Z Kuscsik (2006). A self-adjusted Monte Carlo simulation as a model for financial markets with central regulation. *Physica A: Statistical Mechanics and its Applications*, 361(2), 589–605.
Huang, C-W and SS Narayanan (2017). Deep convolutional recurrent neural network with attention mechanism for robust speech emotion recognition. In *Proc. 2017 IEEE Int. Conf. Multimedia and Expo*, pp. 583–588, Institute of Electrical and Electronics Engineers (IEEE): Hong Kong, China.
Inglada-Perez, LA (2020). Comprehensive framework for uncovering non-linearity and chaos in financial markets: Empirical evidence for four major stock market indices. *Entropy*, 22, 1435.
International Monetary Fund (2021). *Developing Government Bond Markets*. The World Bank. Washington DC, USA. ISBN: 9780821349557. ISSN: 2663-3744.
Issa, G and E Jarnecic (2019). Effect of trading relationships on execution costs in low information asymmetry over-the-counter markets. *Journal of Financial and Quantitative Analysis*, 54(6), 2605–2634.
Klioutchnikov, I, M Sigova and N Beizerov (2017). Chaos theory in finance. *Procedia Computer Science*, 119, 368–375.
Krugman, P (1991). Target zones and exchange rate dynamics. *Quarterly Journal of Economics*, 106, 669–682.
Ma, M and Z Mao (2019). Deep recurrent convolutional neural network for remaining useful life prediction. In *Proc. 2019 IEEE Int. Conf. Prognostics and Health Management (ICPHM)*, pp. 1–4, Institute of Electrical and Electronics Engineers (IEEE): San Francisco, CA.
Neklyudov, A (2019). Bid–ask spreads and the over-the-counter interdealer markets: Core and peripheral dealers. *Review of Economic Dynamics*, 33, 57–84.
O'Shea, K and R Nash (2015). An introduction to convolutional neural networks. arXiv:1511.08458.
Pasquariello, P, J Roush and C Vega (2020). Government intervention and strategic trading in the U.S. Treasury Market. *Journal of Financial and Quantitative Analysis*, 55(1), 117–157.
Pelizzon, L, MG Subrahmanyam, D Tomio and J Uno (2013). The microstructure of the European Sovereign Bond Market: A study of the Euro-zone crisis. *SSRN Electronic Journal*.

Peng, H, J Li, Y Song and Y Liu (2017). Incrementally learning the hierarchical Softmax function for neural language models. In *Proc. Thirty-First AAAI Conf. Artificial Intelligence (AAAI-17)*, pp. 3267–3273.

Pholphirul, P (2009). Macro volatility and financial crisis in Thailand: Some historical evidence. *ASEAN Economic Bulletin*, 26(3), 278–292.

Piesse, J, N Israsena and C Thirtle (2007). Volatility transmission in Asian bond markets: Tests of portfolio diversification. *Asia Pacific Business Review*, 13(4), 585–607.

Qu, H, W Chen, M Niu and X Li (2016). Forecasting realized volatility in electricity markets using logistic smooth transition heterogeneous autoregressive models. *Energy Economics*, 54, 68–76.

Salas, MB, D Alaminos, MA Fernández-Gámez and A Callejón (2020). Forecasting foreign exchange reserves using Bayesian model averaging-naïve bayes. To appear in *The Singapore Economic Review.*

Schlepper, K, H Hofer, R Riordan and A Schrimpf (2020). The market microstructure of central bank bond purchases. *Journal of Financial and Quantitative Analysis*, 55(1), 193–221.

Seyler, E and J Levendis (2015). What was the role of monetary policy in the Greek financial crisis? *South-Eastern Europe Journal of Economics*, 11(2), 117–137.

Stutz, D (2014). Understanding convolutional neural networks. Seminar Report, Fakultat fur Mathematik, Informatik und Naturwissenschaften Lehr-nd Forschungsgebiet Informatik VIII Computer Vision.

Suryani, D, P Doetsch and H Ney (2016). On the benefits of convolutional neural network combinations in offline handwriting recognition. In *Proc. 15th Int. Conf. Frontiers in Handwriting Recognition (ICFHR)*, pp. 193–198, Institute of Electrical and Electronics Engineers (IEEE): Shenzhen, China.

Szegedy, C *et al.* (2015). Going deeper with convolutions. In *Proc. IEEE Conf. Computer Vision and Pattern Recognition*, pp. 1–9, Institute of Electrical and Electronics Engineers (IEEE): Boston, MA.

Tamborini, R (2015). Heterogeneous market beliefs, fundamentals and the sovereign debt crisis in the Eurozone. *Economica*, 82, 1153–1176.

Vu, MT, A Jardani, N Massei and M Fournier (2020). Reconstruction of missing groundwater level data by using long short-term memory (LSTM) deep neural network. *Journal of Hydrology*, 597, 125776.

Wan, L, M Zeiler, S Zhang, YL Cun and R Fergus (2013). Regularization of neural networks using dropconnect. In *Proceedings of 30th Int. Conf. Machine Learning (ICML-13)*, International Conference on Machine Learning (ICML): Atlanta, GA, USA, pp. 1058–1066.

Wang, S, X Chen, C Tong and Z Zhao (2017). Matching synchro squeezing wavelet transform and application to aeroengine vibration monitoring. *IEEE Transactions on Instrumentation and Measurement*, 66, 360–372.

Wihlborg, C, TD Willett and N Zhang (2010). The Euro crisis: It isn't just fiscal and it doesn't just involve Greece. Claremont McKenna College Robert Day School of Economics and Finance Research Paper No. 2011-03. Claremont McKenna College.

Wu, J (2016). *Introduction to Convolutional Neural Networks.* National Key Lab for Novel Software Technology: Nanjing, China.

Yurastika, F and B Wibowo (2021). Volatility spillover between stock and bond returns: Evidence from ASEAN-5 countries. *ICoSMI 2020*, European Alliance for Innovation (EAI): Indonesia.

Zeiler, MD and R Fergus (2014). Visualizing and understanding convolutional networks. In *Proc. European Conf. Computer Vision*, pp. 818–833, Springer: Zurich, Switzerland.

Zhang, Z (2001). Speculative Attacks in the Asian Crisis. Working Paper No. 2001/189, IMF Working Paper. Washington DC, USA.